

## Influence of Doping of Titanium Dioxide by Zirconium and Niobium on its Morphology

L.M. Humeniuk, I.M. Budzulyak, R.V. Ilnytskyk

Vasyl Stefanyk Precarpathian National University, 57, Shevchenka Str., 76000 Ivano-Frankivsk, Ukraine

(Received 16 October 2013; published online 31 January 2014)

Structure porosity and specific surface area of undoped and doped nanodispersed titanium dioxide with Zr, Nb was investigated. The porous structure of  $\text{TiO}_2$  is caused by its intervals between nanoparticles and their agglomerates. Surface morphology of obtained materials was determined by isotherms of nitrogen adsorption-desorption. Specific surface area of nanodispersed titanium dioxide, according to the results, consists 182  $\text{m}^2/\text{g}$ . It was found, that during doping of titanium dioxide with zirconium comparing to origin  $\text{TiO}_2$  specific surface increases in 30 %, and for niobium-doped decreases in 20 %. Pore-size distribution for  $\text{TiO}_2\langle\text{Nb}\rangle$  correspond to the value of 10-15 nm.

**Keywords:** Doping, Titanium dioxide, Specific surface.

PACS number: 68.47.Gh

### 1. INTRODUCTION

Titanium dioxide, especially nanosized  $\text{TiO}_2$ , is a promising material in nowadays technologies [1].  $\text{TiO}_2$  obtaining in different polymorphs (anatase, rutile and brookite) and its modification is a quite topical at this time because it has large specific surface and structure which is capable for intercalation process. Modification of  $\text{TiO}_2$  is mostly done by doping with admixture, which change both the crystal structure and its morphology [2]. This paper presents the study of the pore structure of origin titanium dioxide and its change caused by chemical admixture of transition metals Nb and Zr. We have found [3, 4], that modified in such a way  $\text{TiO}_2$  has a number of advantages, including its larger surface area, smaller particles and better thermal stability [5-7], which is crucial fact for its use as an electrode material [8].

The porous structure of  $\text{TiO}_2$  is caused by its granular structure and it is the intervals between primary and secondary (agglomerates) particles. SEM image of the surface material of  $\text{TiO}_2$ ,  $\text{TiO}_2\langle\text{Zr}\rangle$ ,  $\text{TiO}_2\langle\text{Nb}\rangle$  indicates on a slight increase of spherical grains for  $\text{TiO}_2\langle\text{Nb}\rangle$  [3].

According to data [9], niobium-doping at concentration of 1 %, 3 %, 5 % causes to decrease of  $\text{TiO}_2$  particles for anatase and their increase for rutile. Interacting with each other oxides  $\text{TiO}_2$  and  $\text{ZrO}_2$  form a solid solution  $\text{ZrxTi}_{1-x}\text{O}_2$  with large surface area, high thermal stability and mechanical strength [10].

### 2. EXPERIMENTAL DETAILS

Surface morphology of doped titanium dioxide which main structure is anatase was determined by isotherms of nitrogen adsorption-desorption at a temperature  $T = 77$  K on the device Quantachrome Autosorb (Nova 2200e). Calculation of the specific area and determination of the pore distribution were carried out automatically using computer programs.

Samples were degased in a vacuum chamber with a residual pressure of  $\sim 1.3$  Pa at 373 K for 17 hours. The total pore volume was calculated by volume of adsorbed nitrogen according to desorption isotherm. The method of BJH (Barrett-Joyner-Halendy) was used to determine the porosity. The specific surface area was determined by multipoint method.

### 3. RESULTS AND DISCUSSION

Obtained titanium dioxide by sol-gel technology is nano dispersed with an average particle size of 10 nm. Zirconium and niobium concentration in  $\text{TiO}_2$  was 20 mol % in molar mass, but impurity phases were not observed on X-ray diffractograms [3, 4], indicating its complete solubility in the structure of the main material.

Fig. 1 shows the adsorption-desorption isotherms of nitrogen (a) and pore-size distributions (b) defined by BJH method for the origin  $\text{TiO}_2$ . Isotherm (Fig. 1a) is characterized by two hysteresis loops at relative pressures  $0.4 < P/P_0 < 0.6$  and at  $0.05 < P/P_0 < 0.1$ .

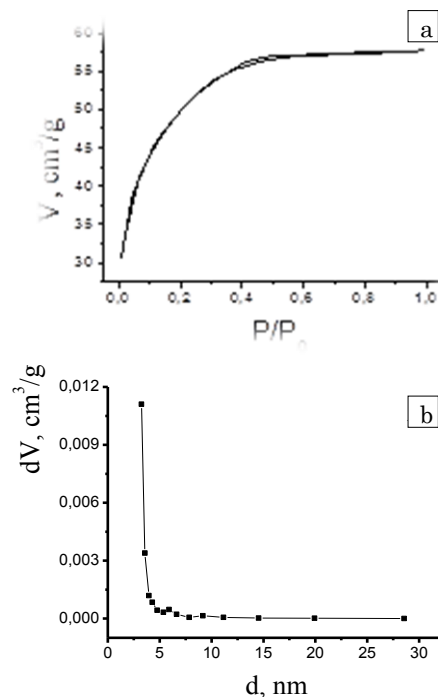


**Fig. 1** –  $\text{N}_2$  isotherms (a) and pore-size distribution (b) for origin  $\text{TiO}_2$

This is a Type I isotherm according to the IUPAC classification, which is inherent for microporous substances and describes the material as a matter of uniform surface, which is consistent with the SEM image, where by the surface of  $\text{TiO}_2$  consists of uniform spherical nanoparticles.

Maximum pore-size distribution for  $\text{TiO}_2$  (Fig. 1b) corresponds to the value of 3 nm. According to the definition of pore size classification this value for  $\text{TiO}_2$  corresponds to micropores as consistent with the obtained isotherm on Fig. 1a.

For niobium-doped titanium dioxide nitrogen isotherm is Type V, which is typical for micro- and mesoporous materials and indicates a significant pore increase after doping.

One explanation for this phenomenon is the increase of nanoparticles surface area or their agglomeration and thus increases of the relative part of the pores with larger size. The value of pore-size distribution for  $\text{TiO}_2(\text{Nb})$  is presented in Fig. 2b.

Comparing with the preceding distribution pore-size distribution in the 10-15 nm region is observed, which corresponds to mesopores, although there are micropores too.

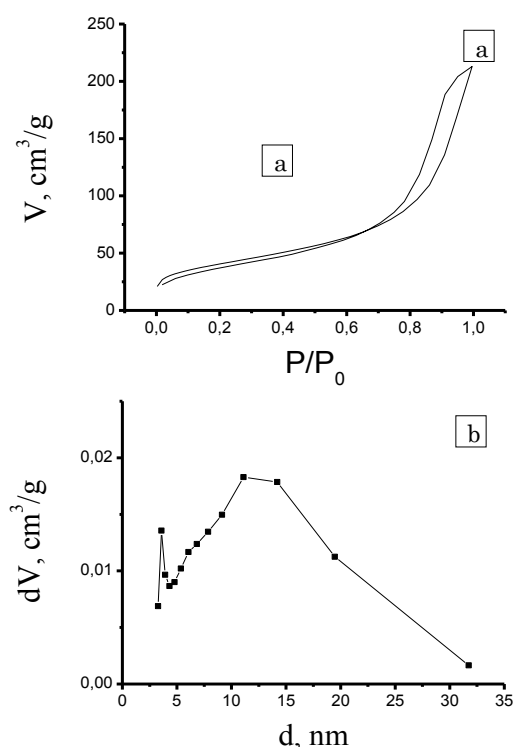


**Fig. 2** –  $\text{N}_2$  isotherms (a) and pore-size distribution for  $\text{TiO}_2$  doped with Nb (b)

For zirconium-doped titanium dioxide (Fig. 3) isotherm indicates an increase in the porosity of the material compared to the origin  $\text{TiO}_2$  and Nb-doped  $\text{TiO}_2$ . For this case it is a type III isotherm, which is close to the V type. Hysteresis loop (Fig. 3a) the same as for previous material at pressures of  $0.8 < P/P_0 < 0.98$  corresponds to filling with nitrogen of major structural pores and mesopores between gaps of agglomerated (secondary) particles. According to Fig. 3b it is clear that the maximum of distribution is for the micropores with the size of 3 nm as to the origin  $\text{TiO}_2$ .

Thus, doping changes the morphology of titanium dioxide, increasing the pore size, especially for the case of  $\text{TiO}_2(\text{Nb})$ . Table 1 shows the parameters of  $\text{TiO}_2$  porous structure.

Especially it is very important that compared with the origin titanium dioxide and  $\text{TiO}_2(\text{Nb})$  specific surface determined by the method of BET and t-method  $\text{TiO}_2(\text{Zr})$  is the largest and corresponds to Fig. 3b.

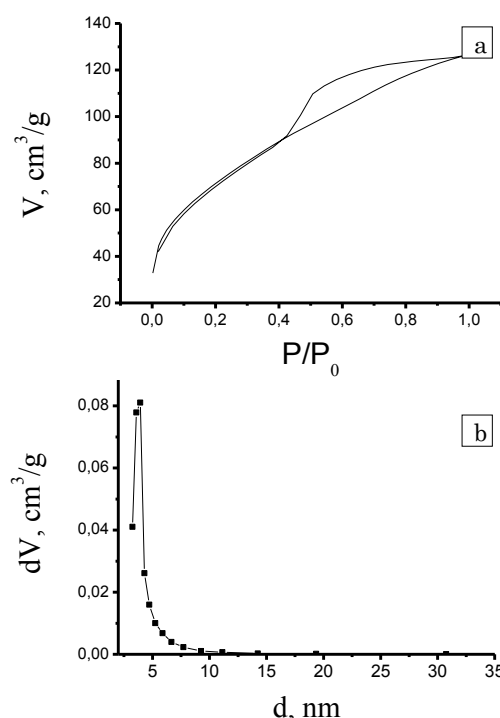


**Fig. 3** –  $\text{N}_2$  isotherms of nitrogen (a) and pore size distribution for Zr-doped  $\text{TiO}_2$  (b)

**Table 1** – Characterization of surface and pore structure of nano dispersed  $\text{TiO}_2$

	$\text{TiO}_2$	$\text{TiO}_2(\text{Nb})$	$\text{TiO}_2(\text{Zr})$
Specific surface area (BET), $\text{m}^2/\text{g}$	182	145	258
Specific surface area (t-method), $\text{m}^2/\text{g}$	132	27,5	67
Specific pore volume, $\text{cm}^3/\text{g}$	0,09	0,33	0,18
Specific pore volume (t-method), $\text{cm}^3/\text{g}$	0,057	0,012	0,029
Average pore size, nm	2	9	3

#### 4. CONCLUSIONS

Pore size and specific surface area of nanodispersed origin, zirconium-and niobium-doped titanium dioxide have been calculated by BJH and BET methods.

It was found that during zirconium-doping specific

surface area increases significantly to 258 m<sup>2</sup>/g relatively to the value for the origin TiO<sub>2</sub> and decreases to 145 m<sup>2</sup>/g for niobium-doped TiO<sub>2</sub>. Micropores are predominant, especially for TiO<sub>2</sub> and TiO<sub>2</sub>(Zr). For TiO<sub>2</sub>(Nb) maximum pore size distribution is 10-15 nm.

#### REFERENCES

1. I.F. Mironyuk, V.O. Kotsyubynskyy, B.K. Ostafiychuk, *Synthesis, structure and electrochemical properties of oxide nanomaterials: a monograph* (Ivano-Frankivsk: Vasyl Stefanyk Precarpathian National University: 2011).
2. A. Zaleska, *Recent patents of engineering* **2**, **57** (2008).
3. L.M. Humeniuk, I.I. Grigorchak, I.M. Budzulyak, R.V. Ilnytskyy, *Phys. Chem. Solids* **13**, **685** (2012).
4. I.M. Budzulyak, L.M. Humeniuk, R.V. Ilnytsky, P.I. Yaremiy, *Visnuk of the Precarpathian University. Chemistry* **2**, **94** (2012).
5. E. Sotter, X. Vilanova, E. Llobet, M. Stankova, X. Correig, *J. Optoelectron. Adv. M.* **7**, 1395 (2005).
6. M.V. Koudriachova, N.M. Harrison, *J. Mater. Chem.* **16**, **1973** (2006).
7. N. Tsvetkov, L. Larina, O. Syevaleevskiy, *Energy Environ. Sci.* **4**, **1480** (2011).
8. A.L. Rahima, The University of Western Ontario London, Ontario, Canada, **265** (2008).
9. P. Sukon, L. Chaikarn, W. Khatcharin, *Sensors* **11**, **472** (2011).
10. M.R. Benjaram, K. Ataulah, *Cataly. Rev.* **47**, **257** (2005).